This is a preprint, the final version is subject to change, of the American Mineralogist (MSA)
Cite as Authors (Year) Title. American Mineralogist, in press.
DOI: http://dx.doi.org/10.2138/am-2018-6208

1 **Revision 1**

2 Water diffusion in silica glass through pathways formed by hydroxyls

3

4 Minami Kuroda[1], Shogo Tachibana[1,2], Naoya Sakamoto[3], Satoshi Okumura[4], Michihiko

5 Nakamura[4] and Hisayoshi Yurimoto[1,3,5]

6

7 [1]Department of Natural History Sciences, Hokkaido University, Sapporo 060-0810, Japan

8 [2]UTokyo Organization for Planetary and Space Science, University of Tokyo, 7-3-1 Hongo,

9 Tokyo 113-0033, Japan

10 [3]Isotope Imaging Laboratory, Hokkaido University, Sapporo 001-0021, Japan

11 [4]Department of Earth Science, Tohoku University, Sendai 980-8578, Japan

12 [5]Institute of Space and Astronautical Science, JAXA, Sagamihara 252-5120, Japan

13 Corresponding author: Minami Kuroda (minami@ep.sci.hokudai.ac.jp)

14

This is a preprint, the final version is subject to change, of the American Mineralogist (MSA)
Cite as Authors (Year) Title. American Mineralogist, in press.
DOI: http://dx.doi.org/10.2138/am-2018-6208

Abstract

Water diffusion in silicate melts is a fundamental process controlling physical and chemical consequences for magmatism, but mechanisms of diffusion in silicate glasses and melts are not fully understood. In this study, water diffusion experiments in silica glass were performed at temperatures of 650°C–850°C and water vapor pressure of 50 bar, with the aim of improving our understanding of the mechanism of water diffusion in a simple SiO_2-H_2O system, and to construct a general water diffusion model for multi-component silicate glasses. Hydrogen diffusion profiles in silica glass were measured by SIMS (Secondary Ion Mass Spectrometry) down to a water concentration of ~10 ppm. Water diffusion profiles indicate that water diffusion becomes slower with decreasing water concentration in silica glass, with the water concentration dependence being greater than in multi-component silicate glasses, particularly at low concentrations (e.g., Doremus 1969, 2000; Zhang and Behrens 2000). A new water diffusion model is proposed for silica glass, where the greater concentration dependence is attributed to the limited number of diffusion pathways in silica glass, formed by breaking Si–O–Si bonds through hydroxyl formation. The model was applied to multi-component silicate glasses, taking into account the effects of metal cations that act as network modifiers by providing additional

diffusion pathways for water molecules. The lower water concentration dependence in multi-component silicate glasses and melts is explained by little dependence of the number of diffusion pathways on water concentration because it is controlled extrinsically by network modifier cations. It is concluded that the number of diffusion pathways is an essential controlling factor for water diffusion in silica and silicate glasses.

Introduction

Water is the most abundant volatile component of magmas. It changes various properties of silicate melts, for example, lowering the viscosity and melting temperature. In volcanic systems, water affects the eruption style through degassing and magma fragmentation due to bubble nucleation and growth in over-saturated ascending magma (e.g., Sparks, 1978). Bubble growth in magma is controlled by viscous relaxation and water diffusion, the relative influences of which depend on magma properties such as temperature, pressure, and chemical composition. Water diffusion in silicate melts is thus one of the important basic parameters controlling the physical and chemical aspects of magmatism.

The diffusion of water in silicate glasses, as a potential analog of silicate melts, has been studied mainly in silica-rich glasses (e.g. Zhang et al., 2007, and references therein). Doremus (1969, 1995) concluded that water diffusivity in silica glass depends linearly on water concentration at 650°C–1000°C, based on published data (Drury et al., 1962; Drury and Roberts, 1963; Roberts and Roberts, 1964, 1966; Burn and Roberts, 1970). This dependence is consistent with that reported by Behrens (2010) for silica glass at 521°C–1097°C at a total pressure of 2 kbar. Tomozawa and co-workers studied water diffusion in silica glass at relatively low water

53 vapor pressures (e.g., Wakabayashi and Tomozawa, 1989; Tomozawa et al., 1994, 2001; Davis
54 and Tomozawa, 1996; Oehler and Tomozawa, 2004), and Wakabayashi and Tomozawa (1989)
55 reported that water diffusion is independent of water concentration in silica glass at 400°C–
56 600°C and 0.5 bar. Regarding silica-rich glasses and melts, Doremus (2000) used literature data
57 (Delaney and Karsten, 1981; Karsten et al., 1982; Laphan et al., 1984) to show a linear
58 concentration dependence of water diffusion in rhyolite melts at 650°C–1000°C and a water
59 vapor pressure of 0.7–5.0 kbar. Zhang and Behrens (2000) showed empirically that water
60 diffusion depends exponentially on water concentration in rhyolite glasses and melts over wide
61 ranges of both temperature and pressure (400°C–1200°C and 0.01–8.1 kbar). Water diffusivities
62 in rhyolite melts and silica glass exhibit a single Arrhenius relationship (Ni et al., 2015) even
63 though their properties (e.g., structural relaxation) differ, implying that data on water diffusion in
64 silicate glasses could potentially be applied to silicate melts with caution.

65 Many diffusion models have been proposed for water diffusion in silicate glasses and
66 melts, but no universal model exists to describe the water diffusion in silicate glasses with
67 various water concentrations and compositions. To elucidate the water concentration dependence
68 of water diffusion in silicate glasses, the present study performed water diffusion experiments in

69 silica glass consisting only of network-forming SiO_4 tetrahedra. The absence of network
70 modifier cations meant that compositional effects could be ignored.
71
72 **Experimental and analytical methods**
73 An optical-quality silica glass plate containing ~10 ppm (~0.0017 mol%) water
74 (SIGMAKOKI Co.), cut into parallelepipeds (5 × 3 × 2 mm), was used as a starting material for
75 water diffusion experiments. In each experiment a silica glass sample and ultrapure water (9.7–
76 11.8 μL) were sealed in a silica glass tube (with 4 mm and 6 mm inner and outer diameters, and
77 80 mm length) in air, and heated in a box furnace at temperatures of 850°C, 800°C, 750°C, and
78 650°C for different periods (Table 1). The amount of water in the sealed tube was adjusted to
79 provide a 50-bar water vapor atmosphere at the set temperatures with complete evaporation of all
80 added water. Experiments were duplicated to confirm results.
81 Concentration profiles of ^{1}H and ^{30}Si were measured using a secondary ion mass
82 spectrometer (SIMS; Cameca ims-6f) at Hokkaido University. The silica glass sample was
83 mounted in Bi–Sn alloy, and the polished cross section was coated with a 70 nm gold layer. A 20
84 nA primary Cs^+ beam was focused to form a 20–30 μm diameter spot on the sample. A field

aperture was used to enable the transmission of ions from the central area (10 μm in diameter) of the sputtered region to minimize the hydrogen signal from absorbed water on the polished sample surface. A normal electron flood gun was used for charge compensation in the sputtered area. Profiles were obtained by moving the sample stage in 5 μm steps across the sample surface. Spatial resolution under this analytical setup was 15–20 μm, corresponding to 3–4 sequential steps of the diffusion profile. Several profiles (usually three) were measured for each sample to assess analytical reproducibility. The position of the diffusion surface was determined as being the point from which ^{30}Si counts became constant. In each analytical session, a calibration curve was made to convert the secondary ion count ratio of $^{1}H/^{30}Si$ to the total water content in the glass using synthetic basalt glasses with known water contents (0, 0.98, and 1.26 mol%), synthesized from natural scoria in a piston cylinder apparatus by S. Yoshimura, Hokkaido University. Hauri et al. (2006) reported that calibration lines for SIMS analysis of water content in silicate glasses do not depend on glass compositions. Hydrogen profiles in the silica glass tube used as the capsule were also determined to evaluate the amount of dissolved water in the tube.

Secondary ion images of ^{1}H and ^{30}Si along the diffusion profile were obtained using an isotope microscope (SCAPS; Stacked CMOS Active Pixel Sensor ion-imaging detector attached

101 to Cameca ims-1270 instrument) at Hokkaido University (Yurimoto et al., 2003). A 1-nA Cs^+
102 primary beam was used for homogeneous irradiation of a sample surface of 50 × 75 μm to
103 extract secondary ions.
104
105 **Results**
106 A typical diffusion profile for a sample heated at 850°C for 25 hours is shown in Fig. 1.
107 The intensity of secondary ^1H decreases from rim to core of the sample, especially rapidly in
108 deeper regions (depth > 180 μm). This rapid decrease is confirmed by secondary ion imaging
109 (Fig. 1, inset). The $^1H/^{30}Si$ ratio profiles obtained from point analyses and isotopic imaging
110 deeper than 180 μm from the surface are consistent (Fig. 1). The rapid decrease in secondary ^1H
111 is therefore not an artefact, but is a feature of diffusive behavior of water in silica glass. No glass
112 crystallization was observed by optical microscopy after the experiments.
113 The $^1H/^{30}Si$ secondary ion intensity ratios were converted to total water concentration in
114 glass using calibration curves produced for each analytical session. Examples of water
115 concentration profiles are given in Fig. 2. A similar degree of water diffusion was observed in
116 the silica glass tube. The total amount of water dissolved in the tube during the diffusion

117 experiments is estimated to be <1% of the initial water in the system, so dissolution in the tube is
118 negligible in the context of this study.
119
120 **Discussion**
121 **Water diffusion model for silica glass**
122 The measured water diffusion profiles do not fit a one-dimensional, semi-infinite
123 diffusion model with fixed surface concentration and constant diffusion coefficient (Crank,
124 1975), which are shown with curve (i) in Fig.2. The curve (i) (Fig. 2) was obtained for water
125 concentrations above certain values (0.2–0.3 wt%) and does not represent diffusion profiles at
126 lower water concentrations. Water diffusivity in silica glass thus depends on the water
127 concentration at 650°C–850°C, with diffusion being slower at lower concentrations.
128 Models with diffusion coefficients having linear or exponential dependence on water
129 concentration (Doremus 1969; Zhang and Behrens 2000s) were applied to silica glass under the
130 same boundary conditions (i.e., one-dimensional, semi-infinite diffusion with a fixed surface
131 concentration; curves (ii) and (iii), Fig. 2), but again these models do not explain the profiles in
132 the low water concentration region. It appears, therefore, that there is a greater concentration

dependence for water diffusion in silica glass than accounted for in previous models proposed for silica and silicate glasses.

Water dissolves in silicate glass as two species, namely molecular water (H_2O_m) and hydroxyls (OH). These interconvert through the following reaction:

$$\mathbf{H_2O_m + O \leftrightarrow 2OH}, \quad (1)$$

where O represents anhydrous oxygen in the glass. The equilibrium constant (K) of reaction (1) is given by

$$\boldsymbol{K = \frac{X_{OH}^2}{X_{H2Om} X_O}}\ , \quad (2)$$

where X_i represents the mole fraction of a single oxygen atom in the species i.

The diffusion coefficient of total H_2O is expressed by the sum of diffusion terms of molecular water and OH (e.g. Ni et al., 2013):

$$\boldsymbol{D_{H_2O_t} = D_{H_2O_m} \frac{\partial X_{H_2O_m}}{\partial X_{H_2O_t}} + D_{OH} \frac{\partial X_{OH}}{2\partial X_{H_2O_t}}} \quad (3)$$

The main diffusive species in silicate glasses is considered to be molecular water (e.g., Doremus 1969; Zhang and Behrens 2000) because hydroxyls are less mobile due to chemical bonding with silicon atoms. Doremus (1999) concluded that the inter-conversion reaction (1) can be at equilibrium in silica glass at temperatures of >650°C. When at equilibrium, with molecular

149 water as the main diffusive species, the diffusion coefficient of total water ($\boldsymbol{D_{H_2O_t}}$) is given by
150 the first term in the product of Equation (3), expressed as a function of the equilibrium constant
151 for the inter-conversion reaction, the total water concentration ($\mathbf{X_{H_2O_t}}$), and the diffusion
152 coefficient of molecular water ($\boldsymbol{D_{H_2O_m}}$):

153 $$\boldsymbol{D_{H_2O_t} = D_{H_2O_m}\left(1-\left(1+\frac{16X_{H_2O_t}}{K}\right)^{-1/2}\right)}. \quad (4)$$

154 It is proposed here that the diffusivity of molecular water ($\boldsymbol{D_{H_2O_m}}$) is controlled not only
155 by jump frequency and distance, but also by the number of diffusion pathways. Molecular water
156 cannot move easily through a polymerized silica glass network, but if a water molecule reacts
157 with silica glass to form two hydroxyls by breaking a Si–O–Si bond (Equation (1)), the
158 hydroxyls can provide a diffusion pathway as shown in Fig. 3. In this case, the number of
159 diffusion pathways would be proportional to half the hydroxyl concentration and $\boldsymbol{D_{H_2O_m}}$ as
160 follows:

161 $$\boldsymbol{D_{H_2O_m} =}$$

162 $$\boldsymbol{[Jump\ frequency\ of\ H_2O_m][Jump\ distance]^2[Number\ of\ diffusion\ pathways] =}$$

163 $$\boldsymbol{vd^2 exp\left(-\frac{E}{RT}\right)\frac{X_{OH}}{2}}, \quad (5)$$

where ν is the molecular vibration frequency that is assumed to be constant, d is the jump distance, E is the activation energy for the jump of molecular water, R is the gas constant, and T is absolute temperature. The jump distance is expected to be constant in the present experiments because the thermal expansion of silica glass is expected to be <0.01% at 650°C–850°C (Narottam and Doremus 1986). In vacancy diffusion in crystals, the number of diffusion pathways should be replaced with the concentration of point defects (Shewmon, 1989).

By combining all concentration-independent factors into D^*, the diffusion coefficient of molecular water can be given by:

$$\boldsymbol{D_{H_2O_m}} = \boldsymbol{D^*}\frac{\boldsymbol{X_{OH}}}{\boldsymbol{2}} \quad (6)$$

The concentration of hydroxyls (X_{OH}) is a function of the total water content (Equation (2)), so $\boldsymbol{D_{H_2O_t}}$ can be written as a function of K and total water content:

$$\boldsymbol{D_{H_2O_t}} = \frac{\boldsymbol{D^*K}}{\boldsymbol{8}}\left(\left(\boldsymbol{1}+\frac{\boldsymbol{16X_{H_2O_t}}}{\boldsymbol{K}}\right)^{\frac{\boldsymbol{1}}{\boldsymbol{2}}}-\boldsymbol{1}\right)\left(\boldsymbol{1}-\left(\boldsymbol{1}+\frac{\boldsymbol{16X_{H_2O_t}}}{\boldsymbol{K}}\right)^{-\frac{\boldsymbol{1}}{\boldsymbol{2}}}\right). \quad (7)$$

In the low water concentration case, $\boldsymbol{D_{H_2O_t}}$ can be approximated as

$$\boldsymbol{D_{H_2O_t}} \approx \frac{\boldsymbol{8D^*}}{\boldsymbol{K}}\boldsymbol{X^2_{H_2O_t}}. \quad (8)$$

Equation (8) clearly shows that there should be greater water concentration dependence for $\boldsymbol{D_{H_2O_t}}$ in silica glass than in models proposed for other silicate glasses and melts, where the

water diffusion coefficient increases linearly or exponentially with concentration (e.g., Doremus, 1969; Zhang and Behrens, 2000). As indicated in the approximation for $\boldsymbol{D_{H_2O_t}}$, appropriate values for D^* and K cannot be found independently through least squares fitting of experimental diffusion profiles. D^* was estimated using K values from Zhang and Ni (2010), where K was reported for rhyolite glass in the temperature range used in the present study, because there is no reported K value for silica glass, and it could not be determined by spectroscopy here due to the very low abundance of molecular water. The K values (Zhang and Ni, 2010) give a concentration ratio of molecular water to hydroxyls of <0.01 in silica glass samples, which is consistent with the lack of molecular water detected in the present study.

The resulting diffusion profiles, fitted with the diffusion coefficient given by Equation (7) in a one-dimensional, semi-infinite diffusion model with a fixed surface concentration, are shown in Fig. 2. This model for total water diffusion better explains the diffusion profiles over a wider range of water concentration than previous models.

Mean values of D^*, obtained from multiple line analyses of a single sample, are summarized in Table 1. The Arrhenius plot (Fig. 4) of D^* at 850°C–750°C indicates that D^* satisfies the Arrhenius relationship with an activation energy of 110 ± 27 kJ/mol, consistent with

196 the activation energy of 60–120 kJ/mol for water diffusion in silicate glasses reported in previous
197 studies (Zhang et al., 2007, and references therein).

198 The D^* value at 650°C was not included in the determination of activation energy
199 because the diffusion profile at 650°C was less well-defined by the present diffusion model, and
200 the diffusion coefficient at that temperature had a larger uncertainty than those at higher
201 temperatures. This is most likely because equilibrium is not achieved in the inter-conversion
202 reaction (Equation (1)) at 650°C (Doremus, 1999).

203

204 **Application to water diffusion in silicate glasses**

205 The water diffusion model for silica glass was applied to diffusion in silicate glasses.
206 Metal cations such as Na, K, Mg, and Ca are present in multi-component silicate glasses. Some
207 of these cations act as "network-modifiers" and some act as "compensating ions" along with Al
208 depending on the concentration of Al and metal cations (Greaves and Ngai, 1995). The
209 network-modifier cations break Si–O–Si bonds to form non-bridging oxygen atoms, resulting in
210 the formation of diffusion pathways for molecular water (Fig. 3). Considering the number of

diffusion pathways formed by network-modifier cations, the diffusivity of molecular water in silicate glasses is given by

$$\boldsymbol{D_{H_2O_m} = \nu d^2 exp\left(-\frac{E}{RT}\right)\left(\frac{X_{OH}}{2} + kX_{NBO}\right)}, \quad (9)$$

where X_{NBO} represents the molar fraction of non-bridging oxygen atoms generated by metal cations and k is the factor to relate the fraction of diffusion pathway to X_{NBO}. Equation (9) explains the weaker water-concentration dependence of water diffusion observed in multi-component silicate glasses and melts (e.g.,Doremus, 1969; Zhang and Behrens, 2000) than in silica glass. At low water concentrations ($\boldsymbol{\frac{X_{OH}}{2} \ll X_{metal}}$) the number of diffusion pathways in silicate glasses ($\boldsymbol{\frac{X_{OH}}{2} + kX_{NBO}}$) is determined primarily by network modifiers, irrespective of water concentration (Fig. 5a). This makes $\boldsymbol{D_{H_2O_m}}$ constant in silicate glasses at low water concentrations (Equation (9); Fig. 5b) and results in an almost linear water concentration dependence of $\boldsymbol{D_{H_2O_t}}$ (Equation (4); Fig. 5c). On the other hand, diffusion pathways in silica glass are formed only by water molecules, as discussed above, and they decreases with decreasing the water concentration (Fig. 5a). Thus, water diffusion in silica glass has greater water concentration dependence because the number of diffusion pathways is intrinsically determined by H_2O itself (Equation (7); Fig. 5c).

227 At higher water concentrations ($\frac{X_{OH}}{2} \gtrsim X_{metal}$), OH also contributes to the formation of
228 diffusion pathways in silicate glasses (Fig. 5a) and $D_{H_2O_m}$ becomes dependent on water
229 concentration (Fig. 5b). The water concentration dependence of $D_{H_2O_t}$ becomes stronger than a
230 simple linear dependence (Fig. 5c), possibly explaining the exponential concentration
231 dependence of water diffusion observed in rhyolite glasses and melts (e.g. Zhang and Behrens,
232 2000).

233 Wakabayashi and Tomozawa (1989) reported concentration-independent water diffusion
234 in silica glass at 400°C–600°C and 0.5 bar. They observed diffusion behavior that seems
235 inconsistent with the strong water-concentration dependence found in the present study, but can
236 be explained by OH diffusion in the glass. Equations (7) and (8) indicate that under extremely
237 low $X_{H_2O_t}$ conditions, the contribution of hydroxyl diffusion may not be negligibly small.
238 Equation (7) can be rewritten as follows when including the OH diffusion term:

$$D_{H_2O_t} = \frac{D^* K}{8}\left(\left(1+\frac{16X_{H_2O_t}}{K}\right)^{\frac{1}{2}}-1\right)\left(1-\left(1+\frac{16X_{H_2O_t}}{K}\right)^{-\frac{1}{2}}\right)$$

239 $$+D^*_{OH}(1-2X_{H_2O_t})\left(4X_{H_2O_t}(X_{H_2O_t}-1)\left(1-\frac{4}{K}\right)+1\right)^{-\frac{1}{2}}, \quad (11)$$

This is a preprint, the final version is subject to change, of the American Mineralogist (MSA)
Cite as Authors (Year) Title. American Mineralogist, in press.
DOI: http://dx.doi.org/10.2138/am-2018-6208

where $\boldsymbol{D^*_{OH}}$ represents water concentration independent OH diffusion. The second product term in Equation (11) is the same as that in Ni et al. (2013). When $\boldsymbol{X_{H_2O_t}}$ is extremely low, Equation (11) indicates that $\boldsymbol{D_{H_2O_t}}$ can be approximated by $\boldsymbol{D^*_{OH}}$. The experiments by Wakabayashi and Tomozawa (1989) were performed at an H_2O pressure of 0.5 bar, much lower than the present and previous experiments, and they therefore observed OH diffusion in silica glass rather than molecular water diffusion, as they supposed. Their small water diffusion coefficients are also consistent with OH diffusion.

It is therefore concluded that the water diffusion model proposed here, where diffusivity depends on the number of diffusion pathways, explains the concentration dependence of water diffusion in multi-component silicate glasses.

Implications

This study has demonstrated that diffusion of molecular water in silicate glasses is controlled by the number of diffusion pathways, which in turn is controlled by the concentrations of water and network modifier cations. The structural effect should also be inevitable for diffusion of other molecular species in silicate glasses such as CO_2 and Ar, which also control

256 physical and chemical properties of ascending magma and are used as an indicator of magma
257 degassing. The diffusion model presented in this study should be applicable to the water
258 concentration dependence of CO_2 and Ar diffusion in silicate glasses (e.g., Behrens and Zhang,
259 2001; Zhang et al., 2007).

260 It has been empirically shown that the water diffusion coefficient in silicate glasses
261 increases with decreasing glass viscosity (Persikov et al., 2010). As the number of diffusion
262 pathways formed by hydroxyls and network modifier cations affects the structural properties of
263 silicate glass, the diffusion model proposed here may improve our understanding of the effect of
264 viscosity on water diffusion.

265

266 **Acknowledgements**

267 We thank Sachio Kobayashi and Jun Kawano for their help with SCAPS analyses and
268 micro-IR analyses, respectively. We also thank Isao Sakaguchi for constructive suggestions on
269 ion-microprobe analysis and the diffusion model. Careful reviews by Bjorn Mysen and an
270 anonymous reviewer are appreciated. This work was supported by Ministry of Education, Sports,
271 Science and Technology KAKENHI grant.

272

273 **References**

274 Behrens, H. (2010) Ar, CO_2 and H_2O diffusion in silica glasses at 2 kbar pressure. Chemical
275 Geology, 272, 40-48.

276 Burn, I., and Roberts, J.P. (1970) Influence of hydroxyl content on the diffusion of water in silica
277 glass. Physics and Chemistry of Glasses, 11, 106-114.

278 Crank, J. (1975) The Mathematics of Diffusion Second Edition, 414 p. Oxford University Press,
279 Oxford.

280 Davis, K.M., and Tomozawa, M. (1995) Water diffusion into silica glass: structural changes in
281 silica glass and their effect on water solubility and diffusivity. Journal of Non-Crystalline
282 Solids, 185, 202-220.

283 Delaney J.R., and Karsten J.L. (1981) Ion microprobe studies of water in silicate melts.
284 Concentration-dependent water diffusion in obsidian. Earth and Planetary Science
285 Letters, 52, 191-202.

286 Doremus, R.H. (1969) The diffusion of water in fused silica. In J.W. Mitchell et al., Eds.,
287 Reactivity of Solids, p. 667-673. Wiley, New York.

288 Doremus, R.H. (1995) Diffusion of water in silica glass. Journal of Materials Research, 10,
289 2379-2389.

290 Doremus, R.H. (1999) Diffusion of water in crystalline and glassy oxides: Diffusion-reaction
291 model. Journal of Material Research, 14, 3754-3758.

292 Doremus, R.H. (2000) Diffusion of water in rhyolite glass: diffusion-reaction model. Journal of
293 Non-Crystalline Solids, 261, 101-107.

294 Drury, T., and Roberts, J.P. (1963) Diffusion in silica glass following reaction with tritiated
295 water vapor. Physics and Chemistry of Glasses, 4, 79-90.

296 Drury, T., Roberts, G.C., and Roberts, P.J. (1962) Diffusion of "water" in silica glass. Advances
297 in glass technology: technical papers of the VI International Congress on Glass, p.
298 249-255. International Commission on Glass.

299 Greaves, G.N., and Ngai, K.L. (1995) Reconciling ionic-transport properties with atomic
300 structure in oxide glasses. Physical Review B, 52, 6358-6380.

Hauri, E.H., Shaw, A.M., Wang, J., Dixon, J.E., King, P.L., and Mandeville, C. (2006) Matrix effects in hydrogen isotope analysis of silicate glasses by SIMS. Chemical Geology, 235, 352-265.

Karsten J.L., Holloway, J.R., and Delaney J.R. (1982) Ion microprobe studies of water in silicate melts: temperature-dependent water diffusion in obsidian. Earth and Planetary Science Letters, 59, 420-428.

Laphan K.E., Holloway, J.R., and Delaney J.R. (1984) Diffusion of H_2O and D_2O in obsidian at elevated temperatures and pressures. Journal of Non-Crystalline Solids, 67, 179-191.

Narottam, P.B., and Doremus, R.H. (1986) Handbook of Glass Properties, 414 p. Academic Press, New York.

Ni, H., Xu, Z., and Zhang, Y. (2013) Hydroxyl and molecular H_2O diffusivity in a haploandesitic melt. Geochemical et Cosmochemica Acta, 103, 36-48.

Ni, H., Hui, H., and Newman, G.S. (2015) Transport properties of silicate melts, Reviews of Geophysics, 53, 715-744.

315 Oehler, A., and Tomozawa, M. (2004) Water diffusion into silica glass at a low temperature
316 under high water vapor pressure. Journal of Non-Crystalline Solids, 347, 211-219.

317 Persikov, E.S., Newman, S., Bukthiyarov, P.G., Nekrasov, A.N., and Stolper, E.M. (2010)
318 Experimantal study of water diffusion in haplobasaltic and haploandesitic melts.
319 Chemical Geology, 276, 241-256.

320 Roberts, G.J., and Roberts, J.P. (1964) Influence of thermal history on the solubility and
321 diffusion of "water" in silica glass. Physics and Chemistry of Glasses, 5, 26-32.

322 Roberts, G.J., and Roberts, J.P. (1966) An oxygen tracer investigation of the diffusion of "water"
323 in silica glass. Physics and Chemistry of Glasses, 7, 82-89.

324 Shewmon, P.G. (1989) Diffusion in Solids. 246 p. Wiley-TMS.

325 Sparks, R.S.J. (1978) The Dynamics of bubble formation and growth in magmas: a review and
326 analysis. Journal of Volcanology and Geothermal Research, 3, 1-37

327 Tomozawa, M., Li, H., and Davis, K.M. (1994) Water diffusion, oxygen vacancy annihilation
328 and structural relaxation in silica glasses. Journal of Non-Crystalline Solids, 179,
329 162-169.

330 Tomozawa M., Kim, D.L., Agrawal, A., and Davis, K.M. (2001) Water diffusion and surface
331 structural relaxation of silica glasses. Journal of Non-Crystalline Solids, 288, 73-80.

332 Wakabayashi, H., and Tomozawa, M. (1989) Diffusion of water into silica glass at low
333 temperature. Journal of the American Ceramic Society, 72, 1850-1855.

334 Yurimoto, H., Nagashima, K., and Kunihiro, T. (2003) High precision isotope micro-imaging of
335 materials. Applied Surface Science, 203-204, 793-797.

336 Zhang, Y., and Behrens, H. (2000) H_2O diffusion in rhyolitic melts and glasses. Chemical
337 Geology, 169, 243-262.

338 Zhang, Y., and Ni, H. (2010) Diffusion of H, C and O components in silicate melts. Reviews in
339 Mineralogy and Geochemistry, 72, 171-225.

340 Zhang, Y., Xu, Z., Zhu, M., and Wang, H. (2007) Silicate melt properties and volcanic eruptions.
341 Reviews of Geophysics, 45, RG4004.

This is a preprint, the final version is subject to change, of the American Mineralogist (MSA)
Cite as Authors (Year) Title. American Mineralogist, in press.
DOI: http://dx.doi.org/10.2138/am-2018-6208

342 **Table 1**. Experimental conditions and water-concentration independent term (D^*) of water
343 diffusion coefficients in silica glass
344

Run #	T (°C)	Time (h)	D^* (2σ) ($m^2 s^{-1}$)
850-1	850	25	1.38 (±0.20) ×10^{-9}
850-2	850	25	1.35 (±0.10) ×10^{-9}
850_05-1	850	12.5	1.43 (±0.08) ×10^{-9}
850_05-2	850	12.5	1.45 (±0.24) ×10^{-9}
800-1	800	25	7.15 (±0.70) ×10^{-10}
800-2	800	25	7.28 (±0.64) ×10^{-10}
750-1	750	40	4.78 (±0.50) ×10^{-10}
750-2	750	40	4.73 (±0.50) ×10^{-10}
750_05-1	750	20	4.33 (±0.16) ×10^{-10}
750_05-2	750	20	4.72 (±0.50) ×10^{-10}
650-1	650	40	1.48 (±0.04)×10^{-10}
650-2	650	40	1.58 (±0.22) ×10^{-10}
650_05-1	650	20	1.22 (±0.48) ×10^{-10}
650_05-2	650	20	6.78 (±0.25) ×10^{-11}

345
346

Figure 1. Typical water diffusion profile (#850-2; 850°C for 25 h). (a) Secondary ion intensity profiles of ^{1}H and ^{30}Si. ^{1}H signals in the region deeper than ~220 μm from the surface correspond to background signals. (b) $^{1}H/^{30}Si$ profile (triangles) calculated from the profiles shown in (a), normalized to $^{1}H/^{30}Si = 1$ at the diffusion surface. The inset shows a secondary ion image of ^{1}H obtained by isotope microscope from the region deeper than ~170 μm from the surface, and the $^{1}H/^{30}Si$ profile (thick line) obtained from the ^{1}H and ^{30}Si images along the depth scale. The $^{1}H/^{30}Si$ ratios of the image analysis are adjusted by the ratio of $^{1}H/^{30}Si$ for the image and point analyses at 180 μm for comparison.

Figure 2. Water diffusion profiles in silica glass at 850, 800, 750 and 650 °C, at a water pressure of 50 bar. The profiles are fitted with water diffusion models proposed in previous studies (dashed curves) (see details in the text): (i) concentration-independent water diffusion (*Wakabayashi and Tomozawa*, 1989), (ii) water diffusion linearly proportional to water concentration (*Doremus*, 1969), and (iii) water diffusion exponentially proportional to water concentration (*Zhang and Behrens*, 2000). Fitted curves with the present water diffusion model are shown as solid curves. Water concentrations near the surface of glasses seem to increase with decreasing temperature, which is likely due to the temperature dependence of water solubility in silica glass (*Wakabayashi and Tomozawa, 1989*)

Figure 3. Schematic illustrations of the diffusion mechanism of molecular water in (a) silica glass and (b) multi-component silicate glass. Diffusion pathways for molecular water are generated by a hydroxyl formation reaction or network modifier cations

Figure 4. Arrhenius plot of D^* for silica glass. Error bars represent two standard deviations of D^* evaluated from several diffusion profiles in samples heated for different periods. The D^* shows the Arrhenius relation with the activation energy of 110 ± 27 kJ/mol. The D^* at 650 °C (open diamond) was not included to determine the activation energy because the error is much larger compared to those of other plots.

Figure 5. Application of the present diffusion model to water diffusion in silicate glasses, where some metal cations act as network modifiers to form non-bridging oxygen atoms (NBOs). The diagrams show changes in (a) the molar fraction of diffusion pathways normalized to that of

NBO (X_{NBO}), (b) the diffusion coefficient of molecular water ($\boldsymbol{D_{H_2O_m}}$), and (c) the diffusion coefficient of total water ($\boldsymbol{D_{H_2O_t}}$) (solid curves) as a function of the concentration ratio of total water relative to NBO ($\boldsymbol{X_{H_2O_t}/X_{NBO}}$). $\boldsymbol{D_{H_2O_m}}$ and $\boldsymbol{D_{H_2O_t}}$ are normalized to $\boldsymbol{D_{H_2O_m}}$ solely determined by NBOs and $\boldsymbol{D_{H_2O_t}}$ at $\boldsymbol{X_{H_2O_t}/X_{NBO}}$ = 1, respectively. The pathway fraction, $\boldsymbol{D_{H_2O_m}}$, and $\boldsymbol{D_{H_2O_t}}$ determined solely by NBOs and OH are shown as dashed and double-dotted curves, respectively. $\boldsymbol{D_{H_2O_t}}$ determined by OH is equivalent to the water diffusion coefficient in silica glass in this study. K=0.41 (850°C for rhyolite glass (Zhang and Ni, 2010)) and X_{NBO}=0.01 were used for calculation. We confirmed that the values of K and X_{NBO} do not change the plots significantly. k in Equation (9) is assumed to be 1 in this calculation.

This is a preprint, the final version is subject to change, of the American Mineralogist (MSA)
Cite as Authors (Year) Title. American Mineralogist, in press.
DOI: http://dx.doi.org/10.2138/am-2018-6208

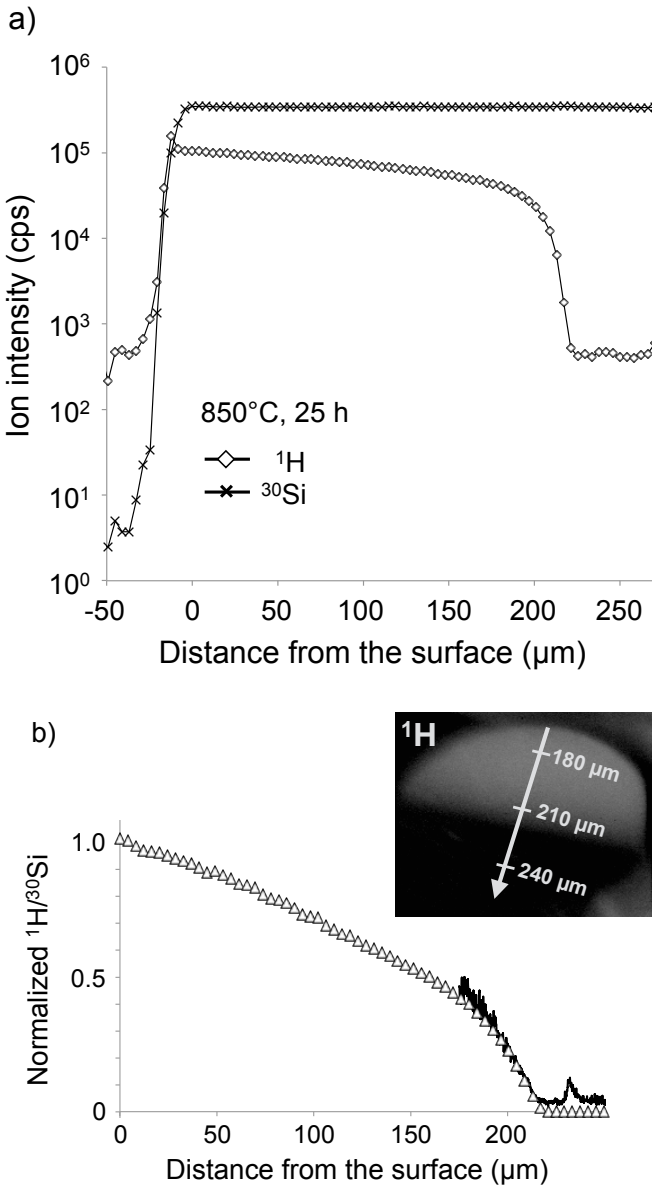

Figure 1.

This is a preprint, the final version is subject to change, of the American Mineralogist (MSA)
Cite as Authors (Year) Title. American Mineralogist, in press.
DOI: http://dx.doi.org/10.2138/am-2018-6208

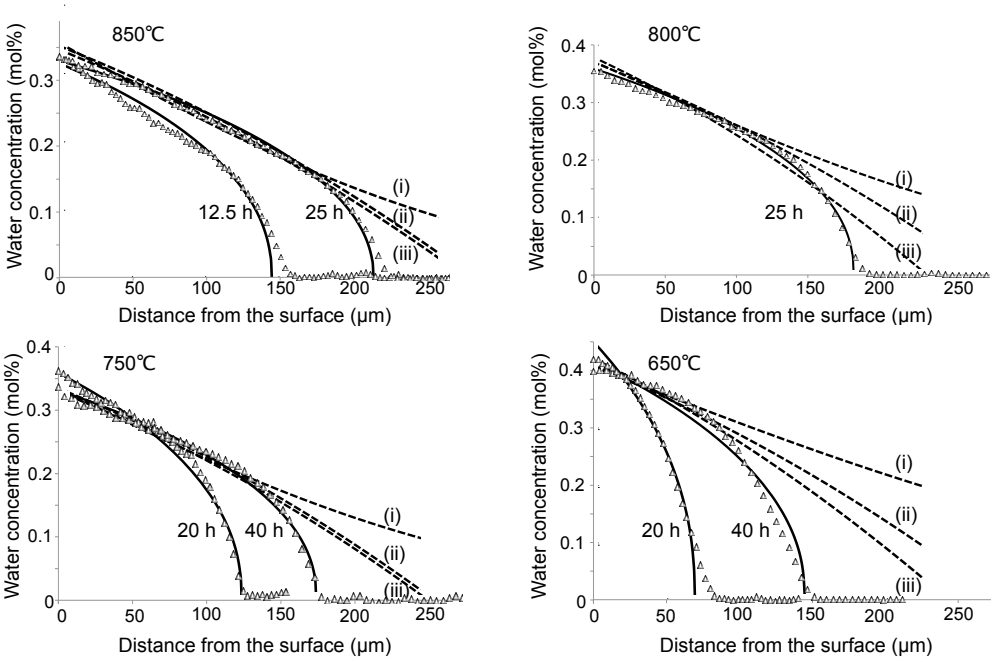

Figure 2.

This is a preprint, the final version is subject to change, of the American Mineralogist (MSA)
Cite as Authors (Year) Title. American Mineralogist, in press.
DOI: http://dx.doi.org/10.2138/am-2018-6208

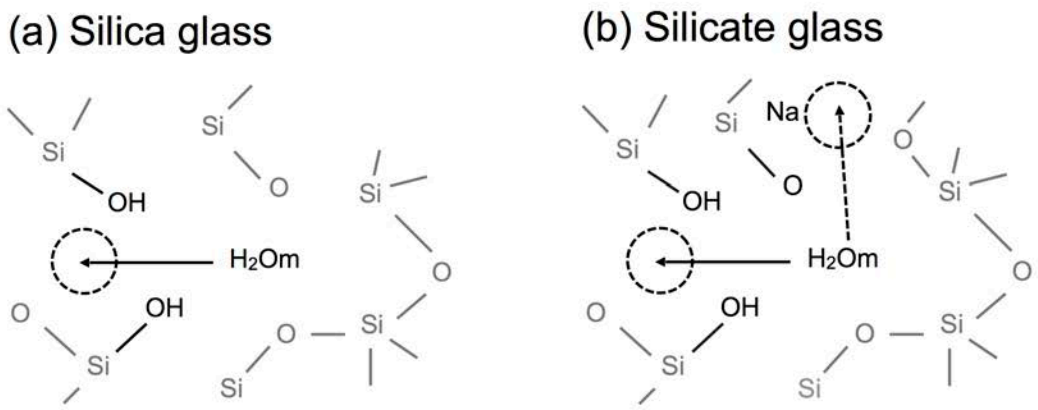

Figure 3.

This is a preprint, the final version is subject to change, of the American Mineralogist (MSA)
Cite as Authors (Year) Title. American Mineralogist, in press.
DOI: http://dx.doi.org/10.2138/am-2018-6208

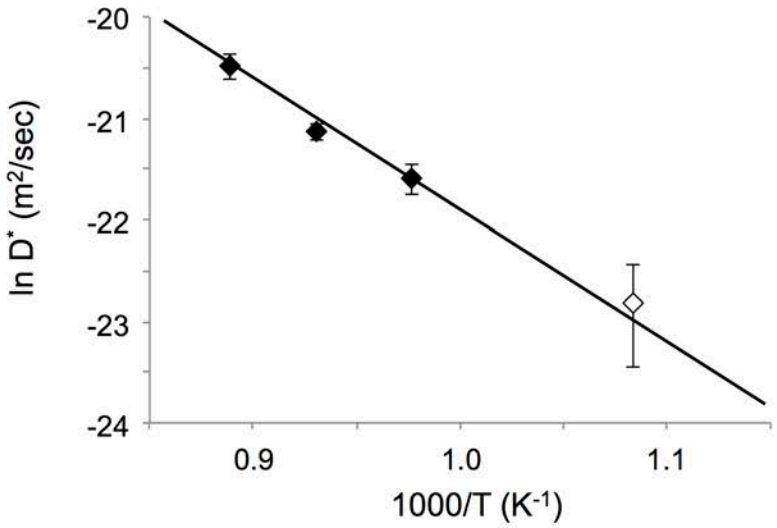

Figure 4.

This is a preprint, the final version is subject to change, of the American Mineralogist (MSA)
Cite as Authors (Year) Title. American Mineralogist, in press.
DOI: http://dx.doi.org/10.2138/am-2018-6208

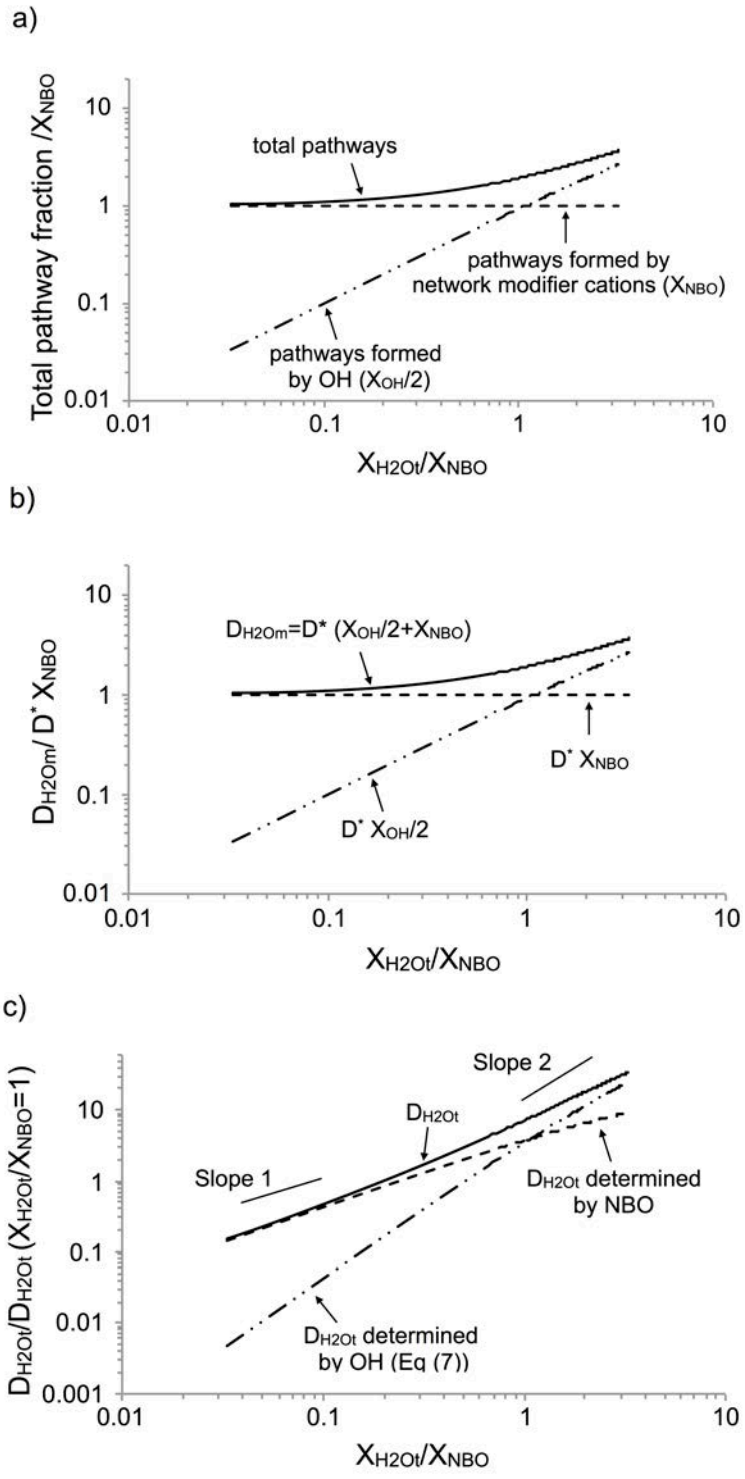

Figure 5.